Amino Acids (2009) 36:99–106
DOI 10.1007/s00726-008-0037-6

ORIGINAL ARTICLE

Mouse and human indoleamine 2,3-dioxygenase display some distinct biochemical and structural properties

Christopher J. D. Austin · Florian Astelbauer · Priambudi Kosim-Satyaputra · Helen J. Ball · Robert D. Willows · Joanne F. Jamie · Nicholas H. Hunt

Received: 30 May 2007 / Accepted: 21 January 2008 / Published online: 15 February 2008

Abstract The hemoprotein indoleamine 2,3-dioxygenase (IDO) is the first and rate-limiting enzyme in the most significant pathway for mammalian tryptophan metabolism. It has received considerable attention in recent years, particularly due to its dual role in immunity and the pathogenesis of many diseases. Reported here are differences and similarities between biochemical behaviour and structural features of recombinant human IDO and recombinant mouse IDO. Significant differences were observed in the conversion of substrates and pH stability. Differences in inhibitor potency and thermal stability were also noted. Secondary structural features were broadly similar but variation between species was apparent, particularly in the α-helix portion of the enzymes. With mouse models substituting for human diseases, the differences between mouse and human IDO must be recognised before applying experimental findings from one system to the next.

Keywords Indoleamine 2,3-dioxygenase · Human · Murine · Thermal stability · pH stability · Kinetics · Inhibiton · Secondary structure

Electronic supplementary material The online version of this article (doi:10.1007/s00726-008-0037-6) contains supplementary material, which is available to authorized users.

C. J. D. Austin (✉) · F. Astelbauer · H. J. Ball · N. H. Hunt
Molecular Immunopathology Unit, Bosch Institute, University of Sydney, Sydney, Australia
e-mail: caustin@mail.med.usyd.edu.au

P. Kosim-Satyaputra · R. D. Willows · J. F. Jamie
Department of Chemistry and Biomolecular Sciences, Macquarie University, Sydney, Australia

Introduction

The first and rate-limiting step of the kynurenine pathway, the major pathway for tryptophan metabolism in humans, is the oxidative cleavage of the 2,3-double bond of the indole ring of tryptophan via the incorporation of molecular oxygen by the heme-containing enzyme indoleamine 2,3-dioxygenase (IDO) (Fig. 1).

IDO is a monomeric, cytosolic protein that is present in most mammalian organs including the intestine, placenta, lung, blood mononuclear phagocytes, epididymis, endocrine and central nervous systems (Heyes and Morrison 1997; Suzuki et al. 2001). IDO has broad substrate specificity and is capable of oxidatively cleaving several indoles including D- and L-tryptophan, tryptamine, 5-hydroxy-L-tryptophan, serotonin and melatonin (Shimizu et al. 1978; Thomas and Stocker 1999). Mouse IDO is 407 amino acids in length, with a molecular weight of 45,639 Da. (Habara-Ohkubo et al. 1991) and human IDO is 403 amino acids long, with a molecular weight of 45,324 Da. Mouse and human IDO orthologs show 62% sequence identity, (Habara-Ohkubo et al. 1991) (Fig. 2) which is low amongst the kynurenine pathway enzymes (Fig. 1).

Recently, a paralog of human and mouse IDO was discovered and named IDO-2. (Ball et al. 2007) The tissue distribution (primarily in the kidney and epididymis) and tryptophan catabolising activity of IDO-2 is different to IDO (Yuasa et al. 2007). At the present time, the functional role of IDO-2 remains unclear.

Under pathological conditions, IDO is over-expressed as a host immune response to rapidly dividing cells and pathogens, such as parasites, (Hansen et al. 2000; Medana et al. 2003; Hansen et al. 2004; Mitchell et al. 2005) bacteria, (Manuelpillai et al. 2003; Oberdorfer et al. 2003; van der Sluijs et al. 2004) and viruses (Potula et al. 2005;

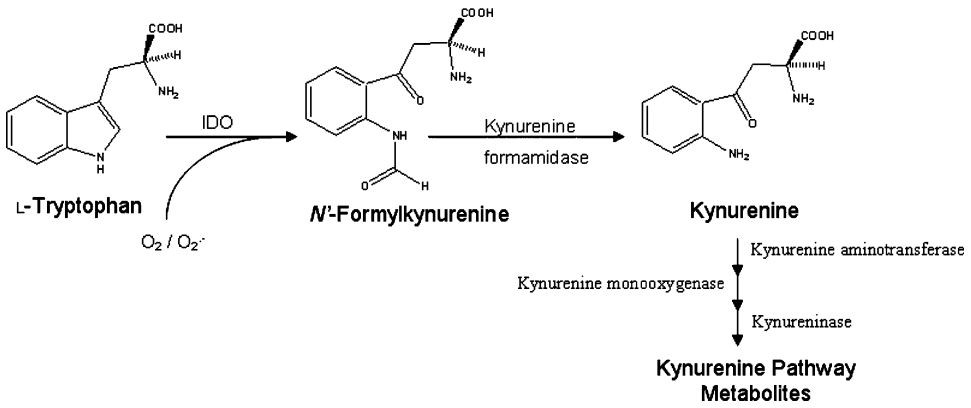

Fig. 1 Initial steps of the kynurenine pathway. The heme containing enzyme indoleamine 2,3-dioxygenase (*IDO*) is capable of catalysing this reaction. The cleavage product, *N*′-formylkynurenine, is then hydrolysed by kynurenine formamidase, (Mouse–Human identity: 69%) or spontaneously, to form kynurenine. Kynurenine is then further metabolised by enzymes of the kynurenine pathway, such, (Mouse–Human identity: 81%) kynurenine monooxygenase, (Mouse–Human identity: 78%) and kynureninase (Mouse–Human identity: 83%) to different metabolic fates

Terajima and Leporati 2005; van der Sluijs et al. 2006). The over-activation of IDO results in the reduction of tryptophan in the cellular environment, depriving cells which pose a challenge to the immune system of this essential amino acid.

The importance of IDO in immunity and disease is increasingly recognised, with mouse models playing a significant role in the study of this influential enzyme. Inhibition of murine IDO has been used to study maternal tolerance of the foetus, a fundamental paradox of the immune system (Munn et al. 1998). Through inhibition of mouse IDO, tryptophan depletion was shown to be essential in preventing the rejection of allogenic conceptii. More recently, mouse IDO inhibition has been shown to potentiate chemotherapy antitumor response, providing important new leads in cancer therapy (Muller et al. 2005a, b; Hou et al. 2007). These and other findings in mouse systems must be interpreted cautiously before application to human models, as no direct comparison of the kinetic and structural features of mouse and human IDO has been performed.

Reported here is a comparative study of the enzymatic behaviour and secondary structural features of recombinant human IDO (rhIDO) and recombinant mouse IDO (rmIDO) allowing greater confidence in the application of results between murine and human systems.

Materials and methods

Subcloning of IDO cDNA from tissue samples

Murine b-end and human HBEC brain endothelial cell lines (courtesy of F. Marelli-Berg and Georges Grau, respectively) were treated with 64 units/ml of interferon gamma overnight. RNA was extracted with 1 ml of Tri reagent (Sigma). Chloroform (0.2 ml) was added, and the lysate was mixed well. After centrifugation at 12,000*g* for 15 min, the aqueous layer was transferred to a new tube. RNAs were precipitated with 500 µl of isopropanol and pelleted at 12,000*g* for 15 min. The pellet was washed with 70% (vol/vol) ethanol and resuspended in water. Genomic DNA contamination was removed by DNase treatment using a DNAfree kit (Ambion). cDNAs were synthesized from up to 2 µg of total RNA in a reaction mixture containing 0.1 µg of oligo(dT)18, 0.6 mmol/L of each nucleotide, 5 U of Prime RNase inhibitor (Eppendorf), and Moloney murine leukemia virus reverse transcriptase (Invitrogen).

Primers were designed based on the previously published sequences of the IDO gene (Human-GenBank® accession number X17668, Mouse-Genbank® accession number NM_008324). The primers for cloning of human IDO had the sequences 5′-CACCATGGCACACGCTATGGAAA-3′ (forward primer) and 5′-TTAACCTTCCTTCAAAAGGGATT-3′ (reverse primer). For mouse IDO, 5′-CACCATGGCACTCAGTAAATATCTC-3′ (forward primer) and 5′-CACTAAGGCCAACTCAGAAGAGCTT-3′ (reverse primer). Both human and mouse IDO forward primers contained a CACC overhang at the 5′ end to allow for directional insertion into pENTR™/D-TOPO® vectors (Invitrogen).

The PCR product was initially ligated into the pENTR™/D-TOPO® vector using the pENTR™/D-TOPO® Cloning Kit (Invitrogen) and transformed into TOP10 *E. coli* cells. Plasmid DNA was isolated from positive colonies, and the human or mouse IDO gene was inserted into pDEST™17 (Invitrogen) via LR recombination reaction. The products were then transformed into DH5α *E. coli* cells, and plasmid DNA that was isolated from the colonies was screened by restriction digestion for incorporation of the IDO gene.

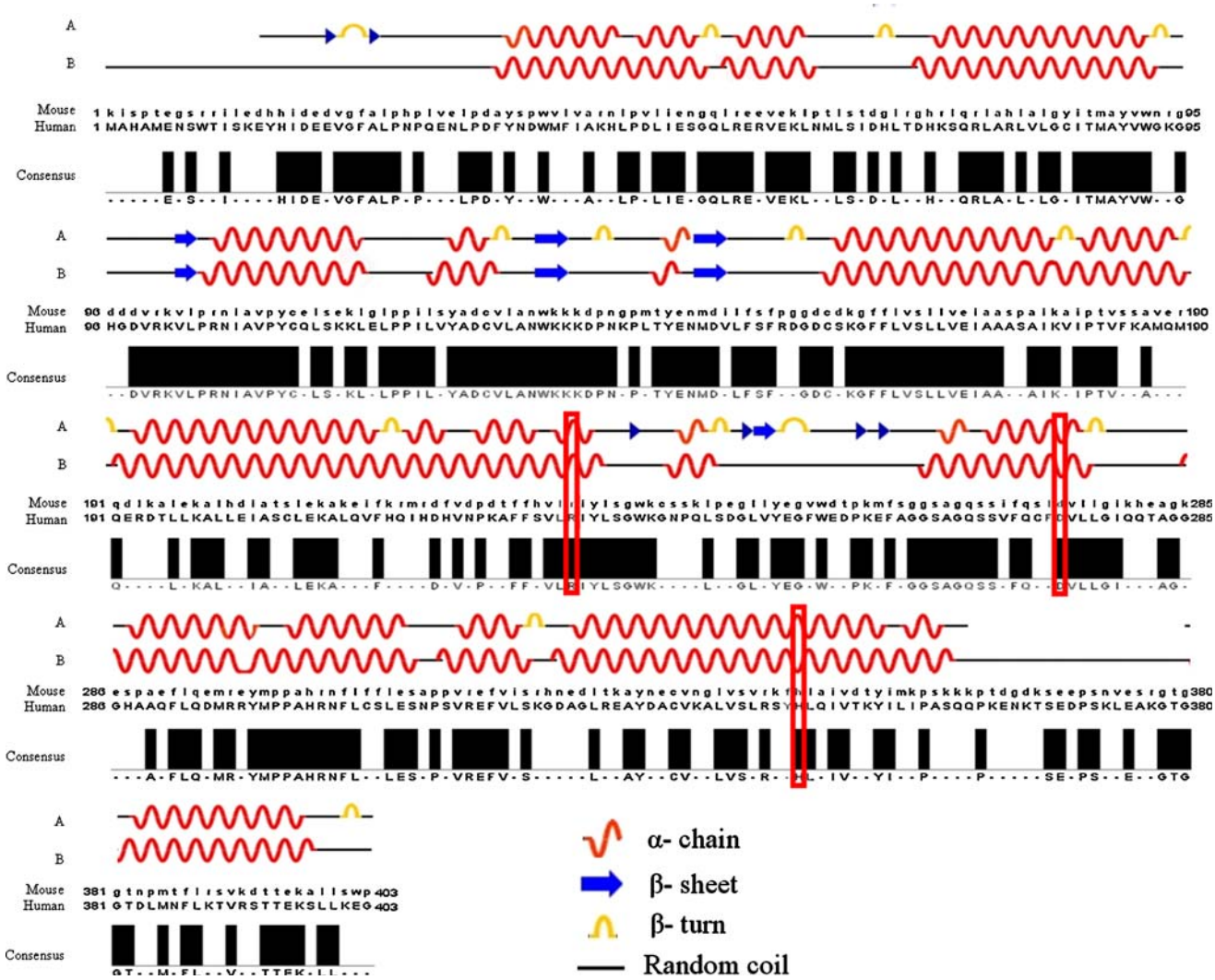

Fig. 2 Sequence alignment of human and mouse IDO. Diagrammatic representation of human IDO secondary structure is shown above the mouse/human sequence alignment—**a** DSSP generated sequence from human IDO crystal structure (Kabsch and Sander 1983) **b** Sugimoto et al. (2006) approved sequence from human IDO crystal structure. Global identity between rmIDO and rhIDO was 62%. Global similarity between rmIDO and rhIDO was 75%. The similarity consensus plot is shown below the sequence alignment. *Red boxes* highlight titratable histidines and carboxylates needed to maintain activity of human IDO

Plasmid DNA isolated from the positive colonies was sequenced to confirm correct incorporation of the gene and to verify the sequence. This plasmid DNA was then used to transform BL21 (DE3) *E. coli* according to the manufacturer's instructions (Invitrogen).

Large-scale expression of recombinant IDO in *E. coli*

BL21 (DE3) *E. coli* transformed with pDEST^{TM}17 plasmid containing human or mouse IDO was grown at 30°C in Luria-Bertani (LB) medium containing 100 μg/mL ampicillin (Sigma). A single colony of BL21 (DE3) IDO positive *E. coli* was inoculated in 100 mL LB medium and cultured overnight. The 100 mL culture was added to 900 mL of the same medium and incubated at 30°C to a density of 0.6 OD at 600 nm. After small scale optimization studies to determine appropriate levels of growth supplements, 1 mM isopropyl *β*-D-1-thiogalactopyranoside (IPTG), 0.2% (*w*/*v*) L-arabinose, 0.5 mM *δ*- aminolevulinic acid (ALA), and 1 mM phenylmethanesulphonylfluoride (PMSF) were then added. Each culture was incubated for a further 3 h. Cells were collected as a pellet by centrifugation at 3,000*g* for 20 min at 4°C. The pellet was suspended in 20 mL ice-cold (Dulbecco's) phosphate–buffered saline (PBS) containing 1 mM PMSF and centrifuged at 3,000*g* for 15 min at 4°C. The pellet was stored at −20°C.

Purification of recombinant IDO (human or mouse)

Frozen pellets from 1 L of bacterial culture, obtained according to the method described earlier, were thawed and suspended in Tris(hydroxymethyl)methylamine (Tris) buffer (25 mM) at pH 7.4, containing NaCl (150 mM), imidazole (10 mM), $MgCl_2$ (10 mM), lysozyme (1 mg/mL), ethylenediaminetetraacetic acid (EDTA) free-cocktail inhibitor tablets (2×, Roche), DNase (<1 mg) and PMSF (1 mM). The resuspended bacterial pellet was incubated on ice for 1 h. The suspension was sonicated (Branson Sonifier, 3 × 40 W, 30 s pulses) before centrifugation at 5,000*g* for 20 min to obtain a clear supernate and pellet.

The clear supernate (25 mL) was then applied to a 1 mL Hi-Trap chelating column (Amersham Biosciences) charged with nickel ions; equilibrated with the basal buffer [Tris (25 mM), pH 7.4; NaCl (500 mM), and PMSF (1 mM)] containing imidazole (10 mM). Following washing with 18 mL of basal buffer, recombinant IDO was eluted at an imidazole concentration of 300 mM, after purification with a stepwise gradient incorporating imidazole concentrations of 50, 65 and 80 mM. The protein collected at the elution step was then buffer exchanged into Tris (50 mM), pH 7.4 using an Amicon Ultra (Millipore) 4 mL centrifugal device with a 30,000 Da molecular weight cut-off, then diluted with a 1:1 addition of 80% glycerol and stored at −80°C.

Protein purity was monitored by sodium dodecyl sulphate-polyacrylamide gel electrophoresis (SDS-PAGE) using a Bio-Rad® Mini-Protean III system according to the method of Laemmli (1970) with some modifications. Proteins were resolved on 12% acrylamide gels and stained with Coomassie Brilliant Blue.

Protein concentration was determined with Bio-Rad® dye reagent (1:5 dilution with MilliQ H_2O) using bovine serum albumin (0–1 mg/mL) as a standard. The coloured product was measured at 595 nm using a SpectraMax 190 micro-plate reader.

Assay of IDO kinetic activity

IDO activity was determined as described by Takikawa et al. (1988) with minor modifications. In brief, the standard reaction mixture (200 µL) contained 50 mM potassium phosphate buffer (pH 6.5), 20 mM ascorbic acid (neutralised with NaOH), 200 µg/mL catalase, 10 µM methylene blue, substrate and IDO (either mouse or human). The reaction was carried out at 37°C for 1 h and stopped by the addition of 40 µL of 30% (*w*/*v*) trichloroacetic acid. After heating at 65°C for 15 min, the reaction mixtures were centrifuged at 11,500*g* for 7 min. The supernate (125 µL) was transferred into a well of a 96-well microtitre plate and mixed with 125 µL of 2% (*w*/*v*) *p*-dimethylaminobenzaldehyde (*p*-DMAB) in acetic acid. The yellow pigment derived from reaction with kynurenine was measured at 480 nm using a SpectraMax 190 microplate reader (Molecular Devices, Sunnyvale, USA). A standard curve of L-kynurenine was used, ranging in concentration from 0 to 500 µM.

Using this assay, the kinetic properties of recombinant human IDO (rhIDO) and recombinant mouse IDO (rmIDO) were determined against three substrates, i.e. L-tryptophan, D-tryptophan and 5-hydroxy-L-tryptophan. Apparent Michaelis-Menten constants (K_m) were determined with varying concentrations of these substrates. The concentration ranges for L-tryptophan, D-tryptophan and 5-hydroxy-L-tryptophan were 5–600, 1–45,000 and 30–4,000 µM, respectively, including carrier controls. Each reaction was conducted in triplicate. Kinetic parameters (K_m, V_{max}) were determined using GraphPad Prism 4 (GraphPad software Inc., CA, USA).

A variation of this assay was used to determine pH stability of rhIDO and rmIDO. Briefly, pH of the 50 mM potassium phosphate buffer, used within the standard reaction mixture, was varied by increments of pH 0.5 over the range pH 6–9. For the pH range 4.1–5.5, 50 mM potassium hydrogen phthalate was used to buffer the reaction mixture. Specific activity of rmIDO and rhIDO was determined using 200 µM L-tryptophan as the substrate.

Comparison of K_i values for competitive and non-competitive inhibitors of IDO

For inhibitor testing, known inhibitors of IDO (Competitive: 1-Methyl-L-Tryptophan (1-MLT); Non-competitive: Norharman) were added to the standard reaction mixture (outlined above) over a concentration range of 50–500 µM with carrier controls. L-Tryptophan substrate concentration was also varied between the ranges 25 and 200 µM with carrier controls. K_i values were determined via non-linear regression analysis using GraphPad Prism 4. The following non-linear regression equations were used with GraphPad Prism: non-competitive, $\{Y = [V_{max}X/(1 + I/K_i)]/K_m + X\}$; and competitive, $K_m(\text{app}) = K_m[1 + I/K]$, $Y = V_{max}X/[K_m(\text{app}) + X]$.

Statistical analysis

Comparisons were performed using a two-way ANOVA statistical analysis followed by a Bonferroni's complementary analysis or Student's *t* test where relevant. *P* values deemed significant are described in figure legends.

Structural analysis of mouse and human recombinant IDO

Circular dichroism (CD) spectra were recorded on a JASCO J-810 spectropolarimeter with 1 mm pathlength quartz cuvettes at a temperature of 20°C. Sensitivity was 100 millidegrees, and the scanning speed was 50 nm/min for an accumulation of 4 scans. CD data were collected between 300 and 190 nm for both human and mouse recombinant IDO at a concentration of 1 mg/mL. Deconvolution of spectra was performed in the CDPro software package (SELCON, CDSSTR, CONTINLL) using a 43 protein reference set (Sreerama and Woody 2000).

Thermal transition curves were measured by monitoring a specific wavelength ($\lambda = 222$ nm or 205 nm) as a function of the increasing temperature over the range 20–99°C at 1°C/min. T_m values were determined by finding the first derivative of the thermal transition curve using peak processing software packaged with the JASCO J-810 spectropolarimeter.

Sequence alignment was performed with CLUSTALW and edited with Jalview. Similarity was determined using the EMBOSS Pairwise Alignment Algorithm (Rice et al. 2000) "needle" utilising the Needleman-Wunsch global alignment algorithm (Needleman and Wunsch 1970).

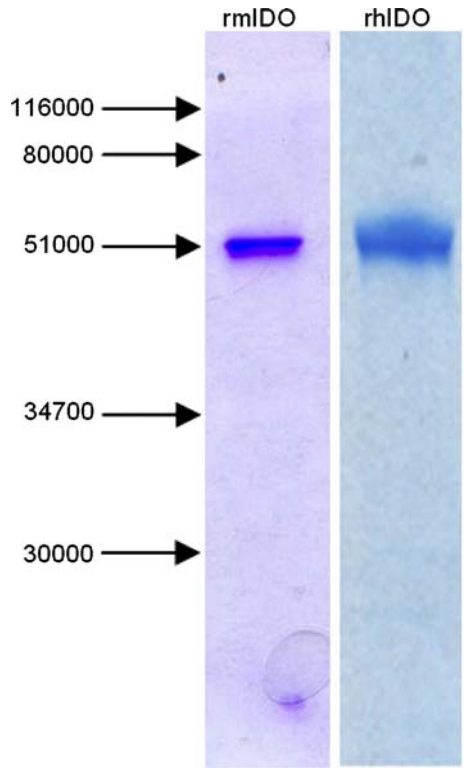

Fig. 3 SDS-PAGE analysis of the eluted rmIDO (*left*) and rhIDO (*right*) taken from Hi-Trap chelating column. The *numbers* on the *left* indicate molecular mass of markers in Daltons

Results and discussion

IDO purity, purification and kinetic activity

Following the purification (Table 1) of the rmIDO and rhIDO proteins, the products obtained were subjected to SDS-PAGE analysis (Fig. 3). As determined by SDS-PAGE, only one homologous band was observed for both isolated proteins with a molecular mass of ~45–50 kDa. pDEST17 clones, including recombinant IDO enzymes investigated in this study, contain a 3.2 kDa N-terminal addition to allow for expression of the 6-His tag. Theoretical molecular weights for recombinant mouse and human IDO are therefore 48.8 and 48.5 kDa, respectively.

The values for K_m and V_{max} are characteristic properties of the enzyme and substrate system. Both rmIDO and rhIDO showed similar activity measurements for L-tryptophan, D-tryptophan and 5-hydroxy-L-tryptophan, with all values appearing within the same order of magnitude. However, significant differences in substrate activity and efficiency were apparent (Table 2) [supplemental data Figs. (a)–(c)].

RmIDO showed a threefold higher substrate efficiency (V_{max}/K_m) ratio than rhIDO when L-tryptophan was used as

Table 1 A summary of purification of rhIDO and rmIDO from the bacterial pellets of 1 L culture of *E. coli* BL21 (DE3), pDEST-17 containing the appropriate IDO gene

IDO type	Step	Volume (mL)	Total protein (mg)	Total activity (μMol/h)	Specific activity of rIDO* (μMol h^{-1} mg^{-1})	Yield (%)	Fold purification
Mouse	Crude extract	20.0	340	4,200	12	100	1
	Hi-Trap	3.50	11	2,387	217	57	18
Human	Crude extract	20.0	354	5,310	15	100	1
	Hi-Trap	3	6.6	1,860	282	35	19

Final samples recovered from the Hi-Trap chelating column gave a single band on SDS-PAGE (Fig. 1). The final recovery for rmIDO and rhIDO was 57 and 35% from the crude extract, respectively. For rmIDO the yield was 3.5 mg/L of growth media. For rhIDO the yield was 3 mg/L of growth media

*Enzyme activity was determined with 200 μM L-tryptophan as the substrate

Table 2 Kinetic and inhibitor parameters of rhIDO and rmIDO for L-tryptophan, D-tryptophan and 5-hydroxy-L-tryptophan at pH 6.5

IDO	L-tryptophan			D-tryptophan			5-hydroxy-L-tryptophan			1-Methyl-L-Tryptophan	Norharman
	V_{max} (min^{-1})	K_m (μM)	V_{max}/K_m (μM^{-1} min^{-1})	V_{max} (min^{-1})	K_m (μM)	V_{max}/K_m (μM^{-1} min^{-1})	V_{max} (min^{-1})	K_m (μM)	V_{max}/K_m (μM^{-1} min^{-1})	K_i (μM)	K_i (μM)
Mouse	203 ± 9	26 ± 4*	7.8	44 ± 2	7300 ± 600	0.006	11 ± 0.3*	210 ± 60*	0.05	105 ± 30	1080 ± 120
Human	198 ± 13	74 ± 15	2.6	44 ± 7	5200 ± 210	0.008	8 ± 0.7	680 ± 160	0.012	62 ± 10	1280 ± 110

Statistical results are expressed as the mean ± standard error of the mean (SEM); mouse versus human: $^*P < 0.05$

substrate, with a significant difference in K_m being noted. A significant difference in both the V_{max} and K_m of 5-hydroxy-L-tryptophan was also observed, with a twofold difference in the V_{max}/K_m ratio. Again, rmIDO had the higher substrate efficiency. For D-tryptophan, neither enzyme displayed a significant difference in kinetic properties.

No significant difference in the inhibitory effects of norharman could be determined between rmIDO (K_i = 1,080 μM) and rhIDO (K_i = 1,280 μM). The K_i of 1-MLT was 105 μM for rmIDO and 62 μM for rhIDO, indicating that 1-MLT is a better inhibitor of rhIDO than rmIDO; however, the observed differences were not significant.

In a biological context, the significant increase in substrate efficiency of rmIDO for L-tryptophan and 5-hydroxy-L-tryptophan indicates that the binding site of rmIDO more readily accepts L-amino acid substrates as does rhIDO. Tryptophan levels in mouse serum are 25% higher than humans (mouse: 104 μmol L^{-1} vs. human: 73 μmol L^{-1}) (Fernstrom and Wurtman 1971; Huang et al. 2002). As a possible adaptation to higher circulating tryptophan levels, due to dietary differences between species, mouse IDO appears to have become more efficient at converting L-tryptophan than human IDO. 1-MLT and norharman inhibited IDO activity in both species, in a similar manner. Interestingly, rmIDO showed no significant difference in down-regulation of activity with the chiral inhibitor, 1-MLT. Despite rmIDO favouring L-amino acid catabolism, it is less able than rhIDO to accommodate the methyl group of 1-MLT, either due to differences in the binding interaction or steric hindrance.

pH stability

The general trend in enzymatic activity was the same for both rmIDO and rhIDO over the pH range studied (pH 4.0–9.0, Fig. 4). At alkaline pH, rhIDO remained significantly more active than rmIDO, as evidenced by a smaller relative drop in specific activity from the maximum (47% for rhIDO, as opposed to 70% for rmIDO) at pH 9.0. Below pH 5.0, rmIDO had significantly higher activity than rhIDO.

The local pH environment, as well as the relative pK_a of amino acid side chains can have a profound effect on the activity of an enzyme in vitro. Mutation studies have shown that titratable histidines and carboxylates, such as His^{346} (the proximal heme ligand), Arg^{231} and Asp^{274} residues are vital in maintaining tryptophan catabolising activity in human IDO (Highlighted in red, Fig. 2) (Littlejohn et al. 2003; Sugimoto et al. 2006). While these groups remain conserved in mouse IDO, the surrounding amino acid environments (especially in the loop containing the proximal heme ligand; Mouse–Human identity: 43%)

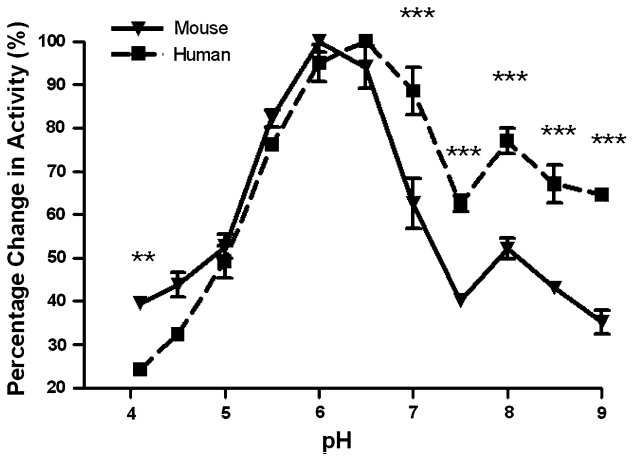

Fig. 4 Graph of pH versus percentage change of maximum activity. RmIDO had a global maximum at pH 6.0; rhIDO had a global maximum at pH 6.5. Statistical results are expressed as the mean ± standard error of the mean (*SEM*); mouse versus human: ** $P < 0.01$, *** $P < 0.001$

lack consensus. The response of these dissimilar structural features to charge may explain the differences in tryptophan catabolising activity observed.

CD spectroscopy: secondary structure analysis

CD spectra were acquired to compare the gross secondary structure of rmIDO and rhIDO (Fig. 5). Far UV CD spectra were analysed using Cdpro (Table 3). The data collated in Table 3 was compared to the available secondary structure data derived from the human IDO crystal (Sugimoto et al. 2006). RhIDO used in this study and crystallised human IDO showed comparable levels of α-helix and β-sheet, giving greater validity to the predicted secondary structure of rmIDO.

The secondary structures of both species were broadly similar, with enzymes being predominantly α-helical, 71 and 61% for rmIDO and rhIDO, respectively. However, the difference in α-helix proportions is large enough to provide

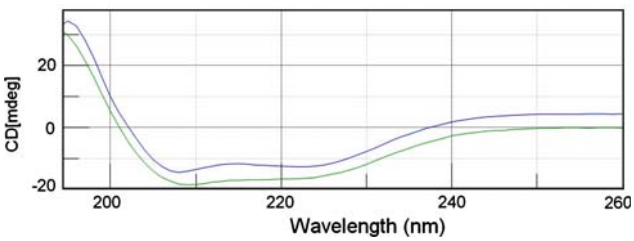

Fig. 5 Circular dichroism analyses of recombinant mouse (*blue line*) and human (*green line*) IDO. Circular dichroism spectra were conducted in 10 mM Tris (pH 7.4) buffer with a 1 mm pathlength cuvette. Protein concentration: 1 mg/mL. The region 195–260 nm is shown

Table 3 Secondary structure analyses of rmIDO and rhIDO

Protein	rmIDO (%)	rhIDO-predicted (%)	RhIDO-observed (Sugimoto et al. 2006)
α-helix	71	61	63%
β-sheet	4	7	1%
β-turn	15	19	ND
Random coil	10	13	ND

ND No data on the percentage of β-turn and random coil

some context for the observed variation in kinetic activity. Experimental data supports the conclusion that rmIDO has a greater preference for L-amino acids molecules with small attached moieties (see "IDO purity, purification and kinetic activity"). Compositional differences around the rmIDO active site, particularly in the amount of α-helix structures, could play a substantial role in the divergence of activity from rhIDO.

CD spectroscopy: thermal unfolding

Thermal denaturations of rmIDO and rhIDO were observed using CD spectrometry. Loss in structure was monitored at $\lambda = 222$ nm (Fig. 6). With over 60% of the IDO protein in both mouse and human species consisting of α-helix structures (Chen et al. 1974), this region was of significant interest. Figure 6 shows the loss of secondary structure of rmIDO and rhIDO as a function of temperature. RhIDO (green line) showed a two state denaturation with intermediates displaying T_m of 48 and 70°C. The T_m of the denaturation process for rmIDO was 60°C, with a possible second intermediate at a T_m of 44°C.

Whilst many physical and kinetic properties of rhIDO and rmIDO show similarities, distinctions in pH, thermal stability, substrate activity and efficiency of these increasingly studied proteins are apparent. With a dependence on mouse models to substitute for human conditions when studying the pathogenesis of disease, the differences between mouse and human IDO must be recognised and accounted for, before applying interpretation of experimental findings from one system to the next.

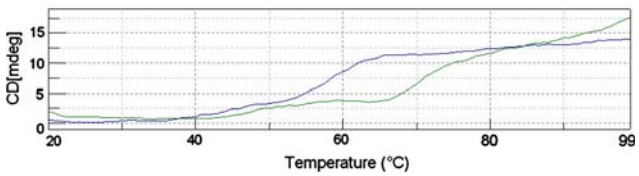

Fig. 6 Thermal transition of rmIDO (*blue*) and rhIDO (*green*) at $\lambda = 222$ nm over the range 20–99°C

Acknowledgments This work was supported by the Australian Research Council and the Sir Zelman Cowen Universities Fund.

References

Ball HJ, Sanchez-Perez A, Weiser S, Austin CJD, Astelbauer F, Miu J, McQuillan JA, Stocker R, Jermiin LS, Hunt NH (2007) Characterization of an indoleamine 2,3-dioxygenase-like protein found in humans and mice. Gene 396:203–213

Chen YH, Yang JT, Chau KH (1974) Determination of helix and beta-form of proteins in aqueous-solution by circular-dichroism. Biochemistry 13:3350–3359

Fernstrom JD, Wurtman RJ (1971) Brain serotonin content—physiological dependence on plasma tryptophan levels. Science 173:149

Habara-Ohkubo A, Takikawa O, Yoshida R (1991) Cloning and expression of a cDNA encoding mouse indoleamine 2,3-dioxygenase. Gene 105:221–227

Hansen AM, Driussi C, Turner V, Takikawa O, Hunt NH (2000) Tissue distribution of indoleamine 2,3-dioxygenase in normal and malaria-infected tissue. Redox Rep 5:112–115

Hansen AM, Ball HJ, Mitchell AJ, Miu J, Takikawa O, Hunt NH (2004) Increased expression of indoleamine 2,3-dioxygenase in murine malaria infection is predominantly localised to the vascular endothelium. Int J Parasitol 34:1309–1319

Heyes MP, Morrison PF (1997) Quantification of local de novo synthesis versus blood contributions to quinolinic acid concentrations in brain and systemic tissues. J Neurochem 68:280–288

Hou DY, Muller AJ, Sharma MD, DuHadaway J, Banerjee T, Johnson M, Mellor AL, Prendergasts GC, Munn DH (2007) Inhibition of indoleamine 2,3-dioxygenase in dendritic cells by stereoisomers of 1-methyl-tryptophan correlates with antitumor responses. Cancer Res 67:792–801

Huang A, Fuchs D, Widner B, Glover C, Henderson DC, Allen-Mersh TG (2002) Serum tryptophan decrease correlates with immune activation and impaired quality of life in colorectal cancer. Br J Cancer 86:1691–1696

Kabsch W, Sander C (1983) Dictionary of protein secondary structure—pattern-recognition of hydrogen-bonded and geometrical features. Biopolymers 22:2577–2637

Laemmli UK (1970) Cleavage of structural proteins during assembly of head of bacteriophage-T4. Nature 227:680–685

Littlejohn TK, Takikawa O, Truscott RJW, Walker MJ (2003) Asp(274) and His(346) are essential for heme binding and catalytic function of human indoleamine 2,3-dioxygenase. J Biol Chem 278:29525–29531

Manuelpillai U, Nicholls T, Wallace EM, Phillips DJ, Guillemin G, Walker D (2003) Increased mRNA expression of kynurenine pathway enzymes in human placentae exposed to bacterial endotoxin. Adv Exp Med Biol 527:85–89

Medana IM, Day NPJ, Salahifar-Sabet H, Stocker R, Smythe G, Bwanaisa L, Njobvu A, Kayira K, Turner GDH, Taylor TE, Hunt NH (2003) Metabolites of the kynurenine pathway of tryptophan metabolism in the cerebrospinal fluid of Malawian children with malaria. J Infect Dis 188:844–849

Mitchell AJ, Hansen AM, Hee L, Ball HJ, Potter SM, Walker JC, Hunt NH (2005) Early cytokine production is associated with protection from murine cerebral malaria. Infect Immun 73:5645–5653

Muller AJ, DuHadaway JB, Donover PS, Sutanto-Ward E, Prendergast GC (2005a) Inhibition of indoleamine 2,3-dioxygenase, an immunoregulatory target of the cancer suppression gene Bin1, potentiates cancer chemotherapy. Nat Med 11:312–319

Muller AJ, Malachowski WP, Prendergast GC (2005b) Indoleamine 2,3-dioxygenase in cancer: targeting pathological immune tolerance with small-molecule inhibitors. Expert Opin Ther Targets 9:831–849

Munn DH, Zhou M, Attwood JT, Bondarev I, Conway SJ, Marshall B, Brown C, Mellor AL (1998) Prevention of allogeneic fetal rejection by tryptophan catabolism. Science 281:1191–1193

Needleman SB, Wunsch CD (1970) A general method applicable to the search for similarities in the amino acid sequence of two proteins. J Mol Biol 48:443–453

Oberdorfer C, Adams O, MacKenzie CR, De Groot CJA, Daubener W (2003) Role of IDO activation in anti-microbial defense in human native astrocytes. Dev Tryptophan Serotonin Metab 527:15–26

Potula R, Poluektova L, Knipe B, Chrastil J, Heilman D, Dou HY, Takikawa O, Munn DH, Gendelman HE, Persidsky Y (2005) Inhibition of indoleamine 2,3-dioxygenase (IDO) enhances elimination of virus-infected macrophages in an animal model of HIV-1 encephalitis. Blood 106:2382–2390

Rice P, Longden I, Bleasby A (2000) EMBOSS: the European molecular biology open software suite. Trends Genet 16:276–277

Shimizu T, Nomiyama S, Hirata F, Hayaishi O (1978) Indoleamine 2,3-dioxygenase—purification and some properties. J Biol Chem 253:4700–4706

Sreerama N, Woody RW (2000) Estimation of protein secondary structure from circular dichroism spectra: comparison of CONTIN, SELCON, and CDSSTR methods with an expanded reference set. Anal Biochem 287:252–260

Sugimoto H, Oda S, Otsuki T, Hino T, Yoshida T, Shiro Y (2006) Crystal structure of human indoleamine 2,3-dioxygenase: catalytic mechanism of O_2 incorporation by a heme-containing dioxygenase. Proc Natl Acad Sci USA 103:2611–2616

Suzuki S, Tone S, Takikawa O, Kubo T, Kohno I, Minatogawa Y (2001) Expression of indoleamine 2,3-dioxygenase and tryptophan 2,3-dioxygenase in early concepti. Biochem J 355:425–429

Takikawa O, Kuroiwa T, Yamazaki F, Kido R (1988) Mechanism of interferon-gamma action—characterization of indoleamine 2,3-dioxygenase in cultured human-cells induced by interferon-gamma and evaluation of the enzyme-mediated tryptophan degradation in its anticellular activity. J Biol Chem 263:2041–2048

Terajima M, Leporati AM (2005) Role of indoleamine 2,3-dioxygenase in antiviral activity of interferon-gamma against vaccinia virus. Viral Immunol 18:722–729

Thomas SR, Stocker R (1999) Redox reactions related to indoleamine 2,3-dioxygenase and tryptophan metabolism along the kynurenine pathway. Redox Rep 4:199–220

van der Sluijs KF, Nijhuis M, Levels H, Jansen HM, van der Poll T, Lutter R (2004) Inhibition of indoleamine-2,3-dioxygenase reduces bacterial outgrowth of *S. pneumoniae* in mice recovered from influenza infection. Immunobiology 209:344

van der Sluijs KF, Nijhuis M, Levels JHM, Florquin S, Mellor AL, Jansen HM, van der Poll T, Lutter R (2006) Influenza-induced expression of indoleamine 2,3-dioxygenase enhances interleukin-10 production and bacterial outgrowth during secondary pneumococcal pneumonia. J Infect Dis 193:214–222

Yuasa HJ, Takubo M, Takahashi A, Hasegawa T, Noma H, Suzuki T (2007) Evolution of vertebrate indoleamine 2,3-dioxygenases. J Mol Evol 65:705–714